Published in final edited form as:
Nature. 2010 April 15; 464(7291): 1043–1047. doi:10.1038/nature08875.

Apcdd1 is a novel Wnt inhibitor Mutated in Hereditary Hypotrichosis Simplex

Yutaka Shimomura[1,*], **Dritan Agalliu**[2,*], **Alin Vonica**[3,*], **Victor Luria**[1,6,*], **Muhammad Wajid**[1], **Alessandra Baumer**[4], **Serena Belli**[5], **Lynn Petukhova**[1], **Albert Schinzel**[4], **Ali H. Brivanlou**[3], **Ben A. Barres**[2,†], and **Angela M. Christiano**[1,6,†]

[1]Department of Dermatology, Columbia University, New York, NY, USA [2]Department of Neurobiology, Stanford University, Stanford, CA, USA [3]The Laboratory of Vertebrate Embryology, The Rockefeller University, New York, NY, USA [4]Institute of Medical Genetics, University of Zurich, Zurich, Switzerland [5]Struttura Semplice Genetica Medica APSS, Trento, Italy [6]Department of Genetics & Development, Columbia University, New York, NY, USA

Abstract

Hereditary hypotrichosis simplex (HHS) is a rare autosomal dominant form of hair loss characterized by hair follicle (HF) miniaturization[1, 2]. Using genetic linkage analysis, we mapped a novel locus for HHS to chromosome 18p11.22, and identified a mutation (L9R) in the *APCDD1* gene in three families. We show that APCDD1 is a membrane-bound glycoprotein that is abundantly expressed in human HFs, and can interact *in vitro* with WNT3A and LRP5, two essential components of Wnt signaling. Functional studies revealed that APCDD1 inhibits Wnt signaling in a cell-autonomous manner and functions upstream of β-catenin. Moreover, APCDD1 represses activation of Wnt reporters and target genes, and inhibits the biological effects of Wnt signaling during both the generation of neurons from progenitors in the developing chick nervous system, and axis specification in *Xenopus* embryos. The mutation L9R is located in the signal peptide of APCDD1, and perturbs its translational processing from ER to the plasma membrane. L9R-APCDD1 likely functions in a dominant-negative manner to inhibit the stability and membrane localization of the wild-type protein. These findings describe a novel inhibitor of the Wnt signaling pathway with an essential role in human hair growth. Since APCDD1 is expressed in a broad repertoire of cell types[3], our findings suggest that APCDD1 may regulate a diversity of biological processes controlled by Wnt signaling.

Address for correspondence: Angela M. Christiano, Ph.D., Departments of Dermatology and Genetics & Development, Columbia University, College of Physicians & Surgeons, 630 West 168th Street VC15 204A, New York, NY 10032, ph:212-305-9565, fx: 212-305-7391, amc65@columbia.edu.
*These authors contributed equally to this work.
†These are senior co-authors.

Supplementary Information is linked to the online version of the paper at www.nature.com/nature.

Accession numbers. APCDD1 mRNA NM_153000, protein NP_694545.

Author Contributions. The study was conceived, designed and supervised by A.M.C.; laboratory work, phenotyping, and sample ascertainment were performed by Y.S., D.A., A.V., V.L., M.W. and A.B.; statistical analyses were performed by L.P.; different aspects of clinical genetics, phenotyping, and mutation screening assays were made by M.W., Y.S., A.B., S.B., A.S., and A.M.C.; and Y.S., D.A., A.V., V.L., A.H.B., B.A.B. and A.M.C. had significant input into experimental design and contributed to the preparation and editing of the manuscript.

Author Information. Reprints and permissions information is available at www.nature.com/reprints. The authors declare no competing financial interests.

Keywords

APCDD1; hereditary hypotrichosis; hair follicle; Wnt inhibitor

Hair follicle (HF) miniaturization is a degenerative process that proportionally reduces the dimensions of the epithelial and mesenchymal compartments, and leads to the conversion of thick, terminal hair to fine, vellus hair4. HF miniaturization is most commonly observed in androgenetic alopecia, but is also characteristic of a rare, autosomal dominant form of hair loss, known as hereditary hypotrichosis simplex1 (HHS; OMIM 146520) (Supplementary Note). To gain insight into the molecular underpinnings of HF miniaturization and identify a gene underlying HHS, we performed a linkage study in two Pakistani families (HHS1 and HHS2) (Figs. 1a-d and S1a-l). After excluding the CDSN locus on chromosome 6[5], we used Affymetrix 10K SNP arrays for genotyping, and linkage analysis using a dominant model yielded a maximum LOD score of Z=4.6 on chromosome 18p11.22 (Fig. S1m). We narrowed the candidate interval to a 1.8 Mb region (Fig. 1e) containing 8 genes, 4 pseudogenes and 3 predicted transcripts (Fig. S1n). Direct sequencing identified a heterozygous mutation 26T>G (L9R) in the signal peptide of the Adenomatosis Polyposis Coli Down-regulated 1 (*APCDD1*) gene (Fig. S1o)[6]. The mutation L9R cosegregated with the disease phenotype in both families, and was absent in 200 unrelated, unaffected controls and in the SNP databases (Fig. S1p; data not shown). Unexpectedly, we identified the identical *APCDD1* mutation in an Italian family with autosomal dominant HHS that had previously been mapped to the same region of chromosome 18p11.22 (Fig. S2)[7], providing independent genetic evidence in support of this finding.

APCDD1 was abundantly expressed in both the epidermal and dermal compartments of the human HF, consistent with a role in HF miniaturization. *APCDD1* mRNA and protein was present in human scalp skin by RT-PCR (Fig. S3a), and a western blot using an APCDD1 antibody (Fig. 1l). APCDD1 mRNA and protein were also highly expressed in the HF dermal papilla (DP), the matrix, and the hair shaft (Fig. 1f-j). Apcdd1 orthologs are conserved throughout vertebrate evolution (Fig. S4a,b), suggesting that a role in mouse[3] and human HF growth emerged recently in mammalian species.

Several lines of evidence led us to postulate that APCDD1 may function as a negative regulator of Wnt signaling, including the observation that it is a direct target gene of Wnt/β-catenin [6]; its similarity in expression pattern with another Wnt inhibitor, Wise[8]; the abundance of Wnt inhibitors in the HF[9]; and the conservation of 12 cysteine residues (Fig. S4a), a structural motif important for interaction between Wnt ligands and their receptors[10,11].

To test if APCDD1 is an inhibitor of Wnt signaling, we first determined if APCDD1 interacts with ligands and receptors of the canonical Wnt pathway. No interaction was found with Fzd2, Fzd8, and Dkk4 (data not shown). In contrast, the extracellular domain of APCDD1 (APCDD1ΔTM) coprecipitated with recombinant tagged forms of Wnt3A and LRP5, two proteins important for HF induction [12] (Figs. 2a, S3b and S5), suggesting that APCDD1 can modulate the Wnt pathway via potential interactions with WNT3A and LRP5 at the cell surface. To determine the effect of APCDD1 on Wnt signaling, we performed TOP/FOP Flash Wnt reporter assays in HEK293T cells. Reporter activity induced by WNT3A alone, or in combination with LRP5/Fzd2, was downregulated ~2-fold by APCDD1 in a dose-dependent manner (Fig. 2b), indicating that APCDD1 inhibits the Wnt/β-catenin pathway.

To determine if APCDD1 can function as a Wnt inhibitor *in vivo*, we selected two systems in which the role of Wnt/β-catenin pathway has been well-defined: neuronal specification in the developing spinal cord[13–15], and axis determination in the frog[16,17]. In the chick spinal cord, a Wnt/β-catenin gradient promotes proliferation of neural progenitors and generation of some neuronal classes[13–15]. Transfection of the Wnt reporter *TOP*::eGFP in the chick neural tube revealed strong activation of the pathway in the dorsal and intermediate progenitors, as previously shown[15]. However, overexpression of APCDD1 strongly reduced eGFP expression levels (Fig. S6a-d), decreased by ~20–30% the number of $Sox3^+$ neural progenitors, as well as various neuronal subtypes of dorsal and ventral origin (Figs. 3a-e and S7a-d). This effect was stronger with mouse Apcdd1, a closer ortholog of the chick protein (Figs. S8a-i and S9a-e). These findings are consistent with the hypothesis that APCDD1 functions as a Wnt inhibitor.

The maternal Wnt pathway is required for the formation of dorsal and anterior structures in early *Xenopus* embryos 18,19. Overexpression of APCDD1 in dorsal blastomeres (n=35) reduced the anterior structures, such as the eyes and cement gland, at the tadpole stage (Fig. 4a,b), consistent with maternal Wnt inhibition. APCDD1 also inhibited transcription of the *Siamois* (*Sia*) reporter gene (Fig. 2c), activated by the maternal Wnt pathway[20]. A zygotic Wnt pathway is subsequently activated on the ventral side of the embryo[21], and its inhibition produces secondary axes with incomplete heads[16,17]. Ventral overexpression of APCDD1 induced secondary axes (n=43, 28% duplicated axes, Fig. 4c,d), consistent with an inhibitory effect on zygotic Wnt signaling. The inhibition of Wnt activity by APCDD1 was also seen in transcription assays with *Wnt8* RNA, but not β-catenin (Fig. 2c), indicating that it acts upstream of β-catenin.

We next investigated which domain of APCDD1 mediates its activity and in which cell APCDD1 exerts its function. First, western blot of APCDD1 expressed in HEK293T cells revealed that the protein is glycosylated and forms a dimer (Figs. 1l and S10a-c). Misexpression of mApcdd1ΔTM (lacking the transmembrane domain) in the chick neural tube mimicked the effects observed with mApcdd1 (Figs. S8j-r and S9f-j), suggesting that the Wnt inhibitory activity resides within the extracellular domain. Secondly, APCDD1 could affect either the signaling cell, by regulating Wnt secretion [22], or the receiving cell. In *Xenopus* transcription assays, *Wnt8* RNA injected in one cell activated the *Sia* reporter in an adjacent cell. *APCDD1* RNA inhibited transcription when coinjected with the *Sia* reporter, but not with *Wnt8* (Fig. 4h), suggesting that APCDD1 inhibits Wnt signaling cell-autonomously in the receiving cell. Finally, since Wt-APCDD1 contains a transmembrane domain (Fig. 1k), and was localized to the plasma membrane (Fig. 2h and Fig. S11a,c,f,i), we tested whether APCDD1 undergoes cleavage to generate a diffusible inhibitor (APCDD1ΔTM), however, it was undetectable in the medium of transfected cells (Fig. S10d). Collectively, these data reveal that APCDD1 is likely a membrane-tethered Wnt inhibitor that acts as a dimer at the surface of the Wnt-receiving cell.

The L9R mutation disrupts the hydrophobic core of the signal peptide critical for co-translational processing (Fig. S4b,c)[23]. We analyzed protein stability and localization by western blotting and immunofluorescence in two cell lines (HEK293T or Bend3.0) transfected with either wild-type (Wt) APCDD1 or two different mutant forms (pathogenic mutation, L9R, and conservative substitution, L9V). Two fragments (68 KDa and 130 KDa) were detected in lysates of the Wt- and the L9V-APCDD1-transfected cells, whereas only a faint 68 KDa fragment was detected in the L9R mutant (Fig. 2f). In addition, Wt- or L9V-APCDD1 protein was localized to the cell membrane, while L9R-APCDD1 was retained within the ER (Figs. 2h,i and S11a-j). Furthermore, unlike the Wt isoform, N-terminally GFP-tagged L9R-APCDD1 could not be cleaved to localize at the membrane (Fig. S11l-n). Finally, when the Wt- and L9R-APCDD1 were co-transfected either in cells or injected into

Xenopus embryos, some Wt protein was degraded (Fig 2e,g), and the rest sequestered in the ER along with the L9R isoform (Figs. 2j,k and S11k,o-q). Therefore, the L9R mutation likely functions in a dominant-negative manner, to destabilize the Wt protein and prevent it from reaching the plasma membrane.

We next tested if the L9R mutation affects APCDD1 protein function *in vivo*. In the chick neural tube, expression of L9R-APCDD1 only weakly inhibited eGFP transcription from the Wnt reporter (Fig. S6e,f), and had no effect on $Sox3^+$ neural progenitors and neuronal subtypes (Figs. 3f-j and S7e-h), in contrast to Wt- or L9V-APCDD1 (Fig. S7m-u). Moreover, L9R-APCDD1 was able to block Wt protein function *in vivo* when they were co-transfected (Figs. 3k-o and S7i-l), indicative of a dominant-negative effect. The same results were observed in *Xenopus*, where the inhibitory effect of Wt APCDD1 on Wnt8-induced transcription was blocked by coexpression of the L9R mutant (Fig. 2d).

We then determined the consequences of *Xenopus* APCDD1 (Xapcdd1) protein depletion on axis formation in *Xenopus* embryos. *Xapcdd1* mRNA is expressed maternally throughout development, with the highest levels in animal (future ectoderm) and marginal (future mesoderm) cells of stage 10 embryos (Fig. S12). Depletion of Xapcdd1 protein with a specific translation-blocking MO oligonucleotide (Fig. S13) resulted in loss of anterior and dorsal structures (Fig. 4e and Table S1). This phenotype was rescued by either injection of MO-resistant 5' mutant *Xapcdd1* RNA, or by *DNWnt8* RNAs (Fig. 4f,g and Table S1), which inhibit zygotic Wnt signaling[24]. Therefore, the loss-of-function phenotype is consistent with ectopic activation on the dorsal side of zygotic Wnt activity, and supports the notion that endogenous APCDD1 is a Wnt inhibitor.

In conclusion, we suggest that APCDD1 may prevent formation of the Wnt receptor complex (Fig. 4i) since it interacts *in vitro* with LRP5 and WNT3A. The L9R mutant is unable to repress Wnt-responsive genes, by trapping the Wt protein in the ER where it may undergo degradation (Fig 4i).

Our findings underscore the requirement for exquisitely controlled regulation of the Wnt signaling pathway in HF morphogenesis and cycling [25]. It is known that forced activation of Wnt signaling exclusively in the epidermis leads to increased hair follicle density and tumors[26,27]. We postulate that in HHS, Wnt signaling is indirectly increased through loss of the inhibitory function of APCDD1 in both the epidermal and dermal compartments of the HF, although the lack of HHS scalp samples precluded us from verifying this assumption. This notion is supported by mice with targeted ablation of another Wnt inhibitor, *Klotho*, which exhibit a reduction in HF density due to indirect upregulation of Wnt signaling and a depletion of HF bulge stem cells[28]. Since APCDD1 is expressed in both epidermal HF cells as well as the dermal papilla, we postulate that the simultaneous deregulation of Wnt signaling in both compartments may lead to the proportional reduction in organ size of the HF, resulting in miniaturization.

Our study provides the first genetic evidence that mutations in a Wnt inhibitor result in hair loss in humans. APCDD1 may be implicated in polygenic HF disorders as well, since it resides within linkage intervals on chromosome 18 in families with androgenetic alopecia[29] as well as alopecia areata[30]. Furthermore, since APCDD1 is expressed in a broad range of cell types[3], our findings raise the possibility that APCDD1 is involved in other Wnt-regulated processes, such as morphogenesis, stem cell renewal, neural development and cancer.

METHODS SUMMARY

Linkage analysis

Genome-wide SNP-based genotyping was performed using the Affymetrix Human Mapping 10K 2.0 Array. Quality control and data analysis was performed with Genespring GT (Agilent software). Briefly, SNPs that violated a Mendelian inheritance pattern were removed from the data set prior to analysis. Haplotypes were inferred from raw genotype data. By analyzing haplotypes rather than individual SNPs, type I error introduced by linkage disequilibrium between markers is mitigated. Finally, haplotypes were analyzed for linkage under the assumption of a fully penetrant disease gene with a frequency of 0.001 transmitted by a dominant mode of inheritance.

Mutation analysis

Using the genomic DNA of the family members, all exons and exon-intron boundaries of *APCDD1* gene were amplified by PCR with the gene-specific primers (Table S2). The PCR products were directly sequenced in an ABI Prism 310 Automated Sequencer, using the ABI Prism Big Dye Terminator Cycle Sequencing Ready Reaction Kit (PE Applied Biosystems). The mutation 26T>G disrupts a *Dde*I restriction enzyme site, which was used to screen the family members and control individuals.

Full Methods and any associated references are available in the online version of the paper at www.nature.com/nature.

METHODS

Clinical details and DNA extraction

Informed consent was obtained from all subjects and approval for this study was provided by the Institutional Review Board of Columbia University. The study was conducted in adherence to the Declaration of Helsinki Principles. Peripheral blood samples were collected from the family members as well as unrelated healthy control individuals of Pakistani and European origin (200 individuals each). Genomic DNA was isolated from these samples using the PUREGENE DNA isolation kit (Gentra System).

Genotyping

Genomic DNA from members of two Pakistani families was amplified by PCR using Platinum® PCR SuperMix (Invitrogen) and primers for microsatellite markers on chromosome 18p11. The amplified products were analyzed on 8% polyacrylamide gels.

Mutation analysis of the *APCDD1* gene

Exon 1 and the adjacent boundary sequences of the *APCDD1* gene were amplified using Platinum® *Taq* DNA Polymerase High Fidelity (Invitrogen). Due to the high G/C content, DMSO (final 5%) and $MgSO_4$ (final 1.6 mM) were added to the PCR reaction. Other exons, as well as the exon-intron boundaries of the *APCDD1* gene, were amplified using Platinum® PCR SuperMix (Invitrogen). Primer sequences are shown in Table S2.

In order to screen for the mutation 26T>G (L9R), a part of exon 1 and intron 1 of the *APCDD1* gene was amplified by PCR using Platinum® *Taq* DNA Polymerase High Fidelity (Invitrogen) and the following primers: forward (5'- CCAGAGCAGGACTGGAAATG-3'), reverse (5'- CGCCAAGGGGACAGTGTAG-3'). The amplified PCR products, 191 bp in size, were digested with *Dde*I at 37°C overnight, and run on 2.0% agarose gels.

Cell culture

HEK293T (human embryonic kidney) and Bend3.0 cells were cultured in Dulbecco's modified Eagle's medium (DMEM; GIBCO) supplemented with 10% fetal bovine serum (FBS; GIBCO), 100 IU/ml penicillin, and 100 μg/ml streptomycin. For transfection experiments in HEK293T cells, dishes were coated with a coating medium containing 0.01 mg/ml of fibronectin (Sigma) and 0.03 mg/ml of type I collagen (Sigma) before seeding the cells in order to prevent detachment of the cells.

Anti-APCDD1 antibodies

A mouse polyclonal anti-human APCDD1 antibody was purchased from Abnova Corporation. This antibody was raised against the full-length human APCDD1 protein. We performed epitope-mapping using three truncated GST-APCDD1 proteins (amino acid (aa) residues 1–171, 166–336, and 331–514), and confirmed that the epitope of the antibody exists between aa residues 166 and 336 of the human APCDD1, which corresponds to the middle portion of the extracellular domain (data not shown). This antibody recognized hair shaft and dermal papilla in human hair follicles (Fig. 1g-j), which finely overlapped with the signals detected by in situ hybridization (Fig. 1f). An affinity-purified rabbit polyclonal anti-mouse Apcdd1 antibody was produced by immunizing rabbits with the synthetic peptide, CQRPSDGSSPDRPEKRATSY (corresponding to the C-terminus of the extracellular domain of the mouse Apcdd1 protein, aa residues 441–459) conjugated to KLH (Pierce, Rockford, IL). This region is completely conserved among mouse and human APCDD1 proteins. The antibody was affinity-purified from the serum using the Sulfolink immobilization column (Pierce). This antibody strongly recognized human APCDD1 protein in western blots and immunofluorescence.

RT-PCR in human scalp skin and plucked hairs

Total RNA were isolated from scalp skin and plucked scalp hairs of healthy control individuals using the RNeasy® Minikit (Quiagen). 2 μg of total RNA was reverse-transcribed with oligodT primers and SuperScript™ III (Invitrogen). The cDNAs were amplified by PCR using Platinum® PCR SuperMix and primer pairs for *APCDD1*, *APCDD1L*, keratin 15 (*KRT15*), *LRP5*, *WNT3A*, and β-2 microglobulin (*B2M*) genes (Table S2). Primers for the *KRT15*, *LRP5*, and *WNT3A* genes were designed as described previously[31,32]. PCR products were run on 1.5% agarose gels.

Expression vectors

cDNA sequences for human APCDD1, WNT3A, CD40, and LRP5 were amplified by PCR using primers and templates shown in Table S2. The amplified products were subcloned into the mammalian expression vector pCXN2.133, a slightly modified version of pCXN2[34] with multiple cloning sites. The expression construct for the full-length human LRP5 was kindly provided by Dr. Patricia Ducy in Columbia University. To generate the expression construct for the mouse Frizzled 2 (mFzd2), the full-length open reading frame of the mFzd2 was purchased from Invitrogen (clone ID 6411627), which was subcloned into the *Not*I sites of the pCXN2.1 vector. In order to introduce a Flag-tag between amino acids 35 and 36 of the APCDD1 protein, N-terminal region of the APCDD1 was PCR-amplified using the forward primer (APCDD1-F-XhoI in Table S2) and a reverse primer (APCDD1-R-Flag-AvrII: 5'-AAAACCTAGGCTTATCGTCGTCATCCTTGTAATCATGAGACCTGCTGTCTGGAT-3'), which was followed by digestion with restriction enzymes *Xho*I and *Avr*II. The C-terminal region of the APCDD1 and the truncated APCDD1 proteins with the C-terminal HA-tag was obtained through digestion of the pCXN2.1-Wt-APCDD1-HA and the pCXN2.1-APCDD1-ΔTM-HA constructs with restriction enzymes *Avr*II and *Nhe*I. These two fragments were ligated with *Avr*II site, and subsequently subcloned into the *Xho*I and

*Nhe*I sites of the pCXN2.1 vector. In order to generate expression constructs for N-terminal GFP-tagged APCDD1 protein, the coding region of the *APCDD1* and the rabbit b-globin 3'-flanking sequences were cut out from the pCXN2.1-APCDD1 constructs with restriction enzymes *Xho*I and *Bam*HI, and subcloned in frame into the pEGFP-C1 vector (Clontech). The templates were also subcloned into the *Xho*I and *Bam*HI sites of pBluescript-SK (−) vector (Stratagene). pGEM *Wnt8* (from R. Harland, U.C. Berkley), the *Sia* luciferase reporter gene (from D. Kimmelman, U. Washington), and pSP36 β-catenin (from B. M. Gumbiner, U. Virginia) have been previously described.

To generate a *Xenopus* expression vector for *Xenopus APCDD1*, we used a full length cDNA clone (BC080377, from Open Biosystems) as template and amplified the open reading frame with the primers shown in Table S2. The PCR product was inserted as ClaI/SalI fragment in CS2+2XHA (A. Vonica), resulting in CS2+Xapcdd1 HA.

The full length mouse Apcdd1 cDNA was amplified by RT-PCR from brain endothelial cells using the First Strand Synthesis Kit and High Fidelity Amplification Kit (Roche Applied Science) with primers shown in Table S2, which was subcloned into pCR®II-TOPO (Invitrogen) and pCAGGS[34] vectors for *in vitro* transcription and chick neural tube electroporations, respectively. The Apcdd1ΔTM isoform containing the extracellular domain of mouse Apcdd1 (aa 1–486) was amplified by PCR from the full length cDNA using primers shown in Table S2 and subcloned into pCAGGS vector for chick electroporation.

Chick neural tube electroporations

The full length WT-APCDD1, L9R APCDD1, L9V APCDD1, mouse Apcdd1 or mApcdd1ΔTM isoform were subcloned into the pCAGGS vector and transfected into the chick neural tube (stage 12–13) together with nGFP vector (pCIG) using *in ovo* electroporation as described[35]. The chick embryos were grown for 3–4 additional days in the 39 °C incubator, fixed with 4% PFA/0.1M phosphate buffer, washed and cryoprotected as described[35] before being processed for *in situ* hybridization or immunofluorescence. For the Wnt reporter assays, the TOP::eGFP reporter (M38 TOP::eGFP from Addgene) was transfected alone or in combination with Wt-APCDD1 or L9R-APCDD1. The chick embryos were grown for 12 hours in the 39 °C incubator, fixed with 4% PFA/0.1M phosphate buffer for 30 minutes, washed and cryoprotected as described[35] before being processed for immunofluorescence.

Cell counts and statistical analysis

Spinal cord $Sox3^+$ progenitors, $Isl1/2^+$ ventral motor neurons, $Isl1/2^+$ dorsal interneurons and $Chx10^+$ V2a interneurons were counted from 8 independent 12um thick sections of chick spinal cord from each transfected embryo. The nucleus stained with the transcription factor was considered one cell for this purpose. The cells were counted from both the electroporated side and the opposite control side. The plots were created using Sigma plot with values representing the mean for each embryo. Statistical significance was determined using the Student t-test.

Transient transfections and western blots in cultured cells and human scalp skin

HEK293T cells or Bend3.0 cells were plated in 60 mm dishes the day before transfection. Expression plasmids of APCDD1 were transfected with FuGENE® 6 (Roche Applied Science) at 60% confluency for HEK293 cells or Targefect_HUVEC for Bend3.0 cells. Total amount of transfected plasmids were adjusted with the empty pCXN2.1 vector. The cells were cultured 48 h after transfection in Opti-MEM (GIBCO). The cells were harvested and homogenized by sonication in homogenization buffer (25 mM HEPES-NaOH (pH 7.4), 10mM MgCl2, 250 mM sucrose, and 1X Complete Mini Protease Inhibitor Cocktail (Roche

Applied Science)). The cell debris was removed by centrifugation at 3,000 rpm for 10 min at 4 °C, and the supernatant was collected as cell lysates. N-glycosidase (PNGase F) treatment and extraction of membrane fraction were performed as described previously33. The cultured medium with 1X Complete Mini Protease Inhibitor Cocktail was centrifuged at 1,500 rpm for 5 min at 4 °C. The supernatant was purified with 0.45 μm syringe filters (Thermo Fisher Science), and concentrated using Amicon Ultra-15 Centrifugal Filter Unit with Ultracel-10 Membrane (Millipore) according to the manufacturer's recommendations. Total cell lysates from human scalp skin were extracted by homogenization in 50 mM Tris-HCl (pH 8.0), 150 mM NaCl, 1.0% NP40, 0.5% sodium deoxycholate, 0.1% SDS, and 1X Complete Mini Protease Inhibitor Cocktail. All samples were mixed with equal amount of Laemmli Sample Buffer (Bio-Rad Laboratories) containing 5% β-mercaptoethanol, boiled at 95 °C for 5 min, and analyzed by 10% SDS-polyacrylamide gel electrophoresis (SDS-PAGE). Western blots were performed as described previously36. The primary antibodies used were rabbit polyclonal anti-HA (diluted 1:4,000; Abcam), rabbit polyclonal anti-APCDD1 (1:20,000), mouse polyclonal anti-APCDD1 (1:1,000; Abnova), mouse monoclonal anti-Flag M2 (1:1,000; Sigma), and rabbit polyclonal anti-β-actin (1:10,000; Sigma).

Wnt reporter assays in HEK293T cells

HEK293T cells were seeded in 12 well dishes the day before transfection. Either 100 ng of TOPFlash (active) or FOPFlash (inactive) Wnt reporter vector (gifts from Dr. Patricia Ducy in Columbia University) was transfected into each well along with constructs for WNT3A (200 ng), Fzd2 (100 ng), LRP5 (100 ng), and/or wild type APCDD1-HA (300 ng or 800 ng) using Lipofectamine 2000 (Invitrogen). A construct for β–galactosidase reporter (100 ng) was also transfected for normalization of transfection efficiency. The cells were lysed 36 h after transfection and the signals were assayed as described previously[9]. The Wnt activity was measured based on the ratio of TOP/FOP luciferase activity. The results represent triplicate determination of a single experiment that is representative a total of five similar experiments.

Co-Immunoprecipitation (Co-IP) assays

Expression plasmids (total 4 μg) were transfected into HEK293T cells seeded on 60 mm dishes with FuGENE® 6 (Roche Applied Science) at 60% confluency. 24 h after the transfection, the cells were harvested and homogenized in lysis buffer (20 mM Tris-HCl (pH 7.5), 137 mM NaCl, 10% Glycerol, 2mM EDTA, 0.5% Triton X, and 1X Complete Mini Protease Inhibitor Cocktail). Total cell lysates were collected by centrifugation at 14,000 rpm for 15 min at 4 °C. The samples were incubated with either mouse monoclonal anti-Flag M2 agarose gel (Sigma) or mouse monoclonal anti-HA agarose gel (Sigma) for 3 h at 4 °C. The agarose beads were washed with lysis buffer for five times. The precipitated proteins were eluted with NuPAGE® LDS Sample Buffer containing Sample Reducing Agent (Invitrogen), incubated at 75 °C for 10 min, and separated on 10% NuPAGE® gels (Invitrogen). Western blots were performed using anti-HA (Abcam) and anti-Flag M2 antibodies (Sigma).

GST pulldown assays

In order to express the GST fusion APCDD1 protein in bacteria, the extracellular domain of the human APCDD1 (aa residues 28–486) was PCR-amplified (Table S2), which was subcloned in-frame into the *Eco*RI and *Xho*I sites of pGEX-4T-3 vector (GE Healthcare Life Sciences). Expression of GST-fusion proteins was induced in DH5α (Invitrogen) by the addition of 0.1 mM isopropyl-β-D-thiogalactopyranoside at 37 °C for 3 h, and the fusion proteins were isolated from bacterial lysates by affinity chromatography with glutathione-Sepharose beads (GE Healthcare Life Sciences). LRP5-EC-Flag, WNT3A-HA, or CD40-

EC-HA were overexpressed in HEK293T cells. GST pulldown assays were performed as described previously[37]. The antibodies used were: rabbit polyclonal anti-GST (1:3,000; Santa Cruz Biotechnology), anti-HA (Abcam) and anti-Flag M2 (Sigma).

In situ hybridization

A part of the human *APCDD1* cDNA (GenBank Accession number, NM_153000: nt. 338–1899) was cloned into pCR®II-TOPO vector (Invitrogen). The antisense and sense DIG-labelled cRNA probes were synthesized from the linearized vectors with T7 and SP6 RNA polymerases (Roche Applied Science), respectively. *In situ* hybridization on dissected human hair follicles was performed following the methods described previously with minor modifications[38]. *In situ* hybridizations on chick spinal cord sections were performed as described[39]. The antisense *mApcdd1* mRNA was generated using the *In vitro* transcription kit (Roche, Indianapolis, IN) with T7 RNA polymerase. The antisense chick *Sim1* mRNA was generated using the T3 RNA polymerase.

Indirect immunofluorescence (IIF)

IIF on cultured cells and fresh frozen sections of individually dissected hair follicles was performed as described previously36. IIF on HEK293T and Bend3.0 cells were performed 48 h after the APCDD1 expression constructs were transfected. For some stainings, cell membrane was labeled with rhodamine-phalloidin (Invitrogen). The primary antibodies used were mouse polyclonal anti-APCDD1 (diluted 1:1,000; Abnova), rabbit polyclonal anti-APCDD1 (1:4,000), rabbit polyclonal anti-pan-cadherin (1:200; Invitrogen), and goat polyclonal anti-calnexin (1:200; Santa Cruz Biotechnology). Immunofluorescence on chick spinal cord sections was performed as described[40]. The monoclonal antibodies against Nkx2.2, Pax6, Pax7, En-1 and Evx1 were purchased from DSHB (Iowa); rabbit anti Olig2 (Chemicon, Billerica MA), rabbit anti-Sox3 (provided by S. Wilson; University of Umea), rabbit anti Chx10, and guinea pig anti Isl1/2, sheep anti GFP (Biogenesis) and mouse anti β3-tubulin (Tuj1; Covance) were used as described40.

Quantitation of subcellular localization of APCDD1 protein

Based on the results of immunofluorescence with rabbit polyclonal anti-APCDD1 antibody in HEK293T cells transfected with APCDD1-expression constructs, we measured the subcellular localization of APCDD1 proteins. The cell outline was visualized using rhodamine-phalloidin (Invitrogen). Images were processed in Image J (http://rsbweb.nih.gov/ij/), splitting the channels. First, the outline of the cell was used to measure the signal within the whole cell. Second, scaling the cell frame down, the signal inside the cell was measured. For each cell, the following values were recorded: 1) the adjusted total signal in the cell (the level of fluorescence, relative to the background); 2) the adjusted signal inside the cell; 3) the adjusted signal in the membrane; and 4) the ratio between adjusted signal in the membrane and inside the cell. The adjusted signal (S_{adj}) was calculated by subtracting the background signal and then normalizing to the background (B) signal levels in an empty area of equal size within the same image. $S_{adj} = (S - B)/B$. For example, a reported signal $S_{adj} = 5$ indicates 5 times stronger than the background41–43. Data are represented as average ± 1 SEM (standard error of the mean). P values are reported using heteroscedastic 2-tailed t-tests, applying the Bonferroni correction to take into account the 3-way comparisons (WT versus L9R; WT versus WT + L9R; L9R versus WT + L9R). All reported values are measured in 20 cells per condition.

Xenopus embryo manipulations

Xenopus laevis embryos were obtained by *in vitro* fertilization, cultured in 0.1X MMR and staged according to Nieuwkoop and Faber[44]. *APCDD1* RNA was produced from the

pBluescript-SK (−)-human APCDD1 constructs using the mMessage Machine *in vitro* T7 transcription kit (Ambion). For full length *xapcdd1* RNA expression, the vector (pCMV-SPORT6) was restricted with *Xba*I and transcribed with the mMessage Machine *in vitro* SP6 transcription kit (Ambion). For *Xapcdd1 HA* expression, CS2+Xapcdd1 HA was restricted with *Not*I and transcribed with the same kit. RNA and reporter DNA injections were done at the 4 cell stage. For the effect of APCDD1 on antero-posterior patterning, *APCDD1* RNA (1 ng) was injected in the marginal zone of both dorsal blastomeres at 4 cell stage. For the ventral effect of APCDD1, one ventral blastomere was injected in the marginal zone at the 4 cell stage[45].

Morpholino oligonucleotide techniques

Translation blocking MO oligonucleotide (AS1 MO) was designed and synthesized by GeneTools, with the sequence: 5'-**T**GGTAGTTCAGCTCCAGAATGTCCT, where the nucleotide in bold is the first one in the open reading frame. The efficiency and specificity of the MO was tested on the full length mRNA (wt Xapcdd1 in Fig. S13) and the Xapcdd1 HA mRNA lacking the 5' UTR to which AS1 MO binds (5' mut Xapcdd1 in Fig. S13). RNA preincubation with MO and *in vitro* translation were performed as described previously[46], using the Promega Reticulocyte Lysate System for translation in the presence of [S35]-Met. MO was injected at the 4 cell stage in both dorsal blastomeres (30 ng), alone or together with *xapcdd1* RNA (300 pg) or *DNWnt8* RNA (300 pg). Embryos were scored for the dorso-anterior index (DAI) at stage 41.

Transcription assays

Injected embryos were collected at stage 9 and processed for luciferase assays (Promega) as described[45]. The *Sia* reporter gene[21] was injected at 100 pg DNA. All assays were in triplicate, and each experiment was repeated three times.

RT-PCR in *Xenopus* embryos

Radioactive RT-PCR was performed as described previously[47]. mRNA was purified from whole embryos, or from fragments cut wit a hair knife, at the indicated stages with RNA-Bee (Tel-Test, Inc.), before reverse transcription with SuperScript III (Invitrogen), using Poly dT as priming oligonucleotide. The primers used for PCR were ODC: sense: 5′ CGAAGGCTAAAGTTGCAG 3′, antisense: 5′-AATGGATTTCAGAGACCA-3′; goosecoid (gsc): sense: 5'-TCTTATTCCAGAGGAACC-3', antisense: 5'-ACAACTGGAAGCACTGGA-3'; Xapcdd1 sense: 5'-CTGGAGCTGAACTACCATGG-3', antisense: 5'-TGACCCTCGATGTTTGGAGGC-3'.

Western Blot in *Xenopus* embryo

Xenopus embryos were injected at the 4 cell stage with 1 ng RNA of wt human APCDD1 alone, or together with L9R mutant RNA (1 ng). Injections also contained 1 ng *LacZ* RNA as loading control. Embryos were retrieved at stage 10, homogenized in NP-40 extract buffer, mixed with LDS sample buffer and run on NuPage 4–12% gels (Invitrogen). After transfer to PVDF membrane, blots were incubated with rabbit polyclonal anti-APCDD1 (1:10,000) or anti-β-Galactosidase (1:1000; ProSci Inc.) antibodies, and stained with ECL Western Blotting Reagent (GE Healthcare).

Supplementary Material

Refer to Web version on PubMed Central for supplementary material.

Acknowledgments

We are grateful to the family members for their participation in this study, and to Helen Lam and Ming Zhang for technical assistance. We appreciate the collaboration and helpful discussions with Dr. Robert M. Bernstein and members of the Christiano laboratory at Columbia University. We thank Drs. Satoshi Ishii (Tokyo University, Japan) and Junichi Miyazaki (Osaka University, Japan) for the supplying pCXN2.1 vector. We thank Drs. Colin Jahoda, Andrew Tomlinson, Adrian Salic, Cassandra Extavour, Richard Vallee, Gilbert Di Paolo and Gerard Karsenty for stimulating discussions and comments on the manuscript, and Dr. Patricia Ducy for generously sharing reagents. This work was supported in part by USPHS NIH grant R01AR44924 from NIH/NIAMS (to A.M.C.). Y.S. is supported by a Research Career Development Award from the Dermatology Foundation. The work in Dr. Ben A. Barres' laboratory (D.A. and B.A.B) was supported by grants from the Myelin Repair Foundation and the National Multiple Sclerosis Society (grant RG 3936A7/1). The work in Dr. Ali H. Brivanlou's laboratory (A.V. and A.H.B.) was supported by NIH grants R01 HD032105 (to A.H.B.) and R03HD057334 (to A.V.).

References

1. Toribio J, Quinones PA. Hereditary hypotrichosis simplex of the scalp. Evidence for autosomal dominant inheritance. Br. J. Dermatol 1974;91:687–696. [PubMed: 4141628]
2. Ibsen HH, Clemmensen OJ, Brandrup F. Familial hypotrichosis of the scalp. Autosomal dominant inheritance in four generations. Acta Derm. Venereol 1991;71:349–351. [PubMed: 1681656]
3. Jukkola T, Sinjushina N, Partanen J. Drapc1 expression during mouse embryonic development. Gene Expr. Patterns 2004;4:755–762. [PubMed: 15465500]
4. Trueb RM. Molecular mechanisms of androgenetic alopecia. Exp. Gerontol 2002;37:981–990. [PubMed: 12213548]
5. Betz RC, et al. A gene for hypotrichosis simplex of the scalp maps to chromosome 6p21.3. Am. J. Hum. Genet 2000;66:1979–1983. [PubMed: 10793007]
6. Takahashi M, et al. Isolation of a novel human gene, APCDD1, as a direct target of the beta-Catenin/T-cell factor 4 complex with probable involvement in colorectal carcinogenesis. Cancer Res 2002;62:5651–5656. [PubMed: 12384519]
7. Baumer A, Belli S, Trueb RM, Schinzel A. An autosomal dominant form of hereditary hypotrichosis simplex maps to 18p11.32-p11.23 in an Italian family. Eur. J. Hum. Genet 2000;8:443–448. [PubMed: 10878665]
8. O'Shaughnessy RF, Yeo W, Gautier J, Jahoda CA, Christiano AM. The WNT signalling modulator, Wise, is expressed in an interaction-dependent manner during hair-follicle cycling. J. Invest. Dermatol 2004;123:613–621. [PubMed: 15373764]
9. Bazzi H, Fantauzzo KA, Richardson GD, Jahoda CA, Christiano AM. The Wnt inhibitor, Dickkopf 4, is induced by canonical Wnt signaling during ectodermal appendage morphogenesis. Dev. Biol 2007;305:498–507. [PubMed: 17397822]
10. Kawano Y, Kypta R. Secreted antagonists of the Wnt signalling pathway. J. Cell Sci 2003;116:2627–2634. [PubMed: 12775774]
11. Nakamura T, Matsumoto K. The functions and possible significance of Kremen as the gatekeeper of Wnt signalling in development and pathology. J Cell. Mol. Med 2008;12:391–408. [PubMed: 18088386]
12. Kishimoto J, Burgeson RE, Morgan BA. Wnt signaling maintains the hair-inducing activity of the dermal papilla. Genes Dev 2000;14:1181–1185. [PubMed: 10817753]
13. Megason SG, McMahon AP. A mitogen gradient of dorsal midline Wnts organizes growth in the CNS. Development 2002;129:2087–2098. [PubMed: 11959819]
14. Lei Q, et al. Wnt signaling inhibitors regulate the transcriptional response to morphogenetic Shh-Gli signaling in the neural tube. Dev. Cell 2006;11:325–337. [PubMed: 16950124]
15. Yu W, McDonnell K, Taketo MM, Bai CB. Wnt signaling determines ventral spinal cord cell fates in a time-dependent manner. Development 2008;135:3687–3696. [PubMed: 18927156]
16. Leyns L, Bouwmeester T, Kim SH, Piccolo S, De Robertis EM. Frzb-1 is a secreted antagonist of Wnt signaling expressed in the Spemann organizer. Cell 1997;88:747–756. [PubMed: 9118218]
17. Wang S, Krinks M, Lin K, Luyten FP, Moos M Jr. Frzb, a secreted protein expressed in the Spemann organizer, binds and inhibits Wnt-8. Cell 1997;88:757–766. [PubMed: 9118219]

18. Niehrs C. Regionally specific induction by the Spemann-Mangold organizer. Nat. Rev. Genet 2004;5:425–434. [PubMed: 15153995]
19. Heasman J. Patterning the early Xenopus embryo. Development 2006;133:1205–1217. [PubMed: 16527985]
20. Brannon M, Gomperts M, Sumoy L, Moon RT, Kimelman D. A beta-catenin/XTcf-3 complex binds to the siamois promoter to regulate dorsal axis specification in Xenopus. Genes Dev 1997;11:2359–2370. [PubMed: 9308964]
21. Smith JC, Price BM, Green JB, Weigel D, Herrmann BG. Expression of a Xenopus homolog of Brachyury (T) is an immediate-early response to mesoderm induction. Cell 1991;67:79–87. [PubMed: 1717160]
22. Kadowaki T, Wilder E, Klingensmith J, Zachary K, Perrimon N. The segment polarity gene porcupine encodes a putative multitransmembrane protein involved in Wingless processing. Genes Dev 1996;10:3116–3128. [PubMed: 8985181]
23. Pidasheva S, Canaff L, Simonds WF, Marx SJ, Hendy GN. Impaired cotranslational processing of the calcium-sensing receptor due to signal peptide missense mutations in familial hypocalciuric hypercalcemia. Hum. Mol. Genet 2005;14:1679–1690. [PubMed: 15879434]
24. Hoppler S, Brown JD, Moon RT. Expression of a dominant-negative Wnt blocks induction of MyoD in Xenopus embryos. Genes Dev 1996;10:2805–2817. [PubMed: 8946920]
25. Blanpain C, Fuchs E. Epidermal homeostasis: a balancing act of stem cells in the skin. Nat. Rev. Mol. Cell Biol 2009;10:207–217. [PubMed: 19209183]
26. Gat U, DasGupta R, Degenstein L, Fuchs E. De Novo hair follicle morphogenesis and hair tumors in mice expressing a truncated beta-catenin in skin. Cell 1998;95:605–614. [PubMed: 9845363]
27. Zhang Y. Activation of beta-catenin signaling programs embryonic epidermis to hair follicle fate. Development 2008;135:2161–2172. [PubMed: 18480165]
28. Liu H. Augmented Wnt signaling in a mammalian model of accelerated aging. Science 2007;317:803–806. [PubMed: 17690294]
29. Hillmer AM, et al. Genome-wide scan and fine-mapping linkage study of androgenetic alopecia reveals a locus on chromosome 3q26. Am. J. Hum. Genet 2008;82:737–743. [PubMed: 18304493]
30. Martinez-Mir A, et al. Genomewide scan for linkage reveals evidence of several susceptibility loci for alopecia areata. Am. J. Hum. Genet 2007;80:316–328. [PubMed: 17236136]
31. Pasternack SM, et al. G protein-coupled receptor P2Y5 and its ligand LPA are involved in maintenance of human hair growth. Nat. Genet 2008;40:329–334. [PubMed: 18297070]
32. Konigshoff M, et al. Functional Wnt signaling is increased in idiopathic pulmonary fibrosis. PLoS ONE 2008;3:e2142. [PubMed: 18478089]
33. Noguchi K, Ishii S, Shimizu T. Identification of p2y9/GPR23 as a novel G protein-coupled receptor for lysophosphatidic acid, structurally distant from the Edg family. J. Biol. Chem 2003;278:25600–25606. [PubMed: 12724320]
34. Niwa H, Yamamura K, Miyazaki J. Efficient selection for high-expression transfectants with a novel eukaryotic vector. Gene 1991;108:193–199. [PubMed: 1660837]
35. Briscoe J, Pierani A, Jessell TM, Ericson J. A homeodomain protein code specifies progenitor cell identity and neuronal fate in the ventral neural tube. Cell 2000;101:435–445. [PubMed: 10830170]
36. Bazzi H, et al. Desmoglein 4 is expressed in highly differentiated keratinocytes and trichocytes in human epidermis and hair follicle. Differentiation 2006;74:129–140. [PubMed: 16533311]
37. Shimomura Y, Aoki N, Ito K, Ito M. Gene expression of Sh3d19, a novel adaptor protein with five Src homology 3 domains, in anagen mouse hair follicles. J. Dermatol. Sci 2003;31:43–51. [PubMed: 12615363]
38. Aoki N, et al. A novel type II cytokeratin, mK6irs, is expressed in the Huxley and Henle layers of the mouse inner root sheath. J. Invest. Dermatol 2001;116:359–365. [PubMed: 11231308]
39. Schaeren-Wiemers N, Gerfin-Moser A. A single protocol to detect transcripts of various types and expression levels in neural tissue and cultured cells: in situ hybridization using digoxigenin-labelled cRNA probes. Histochemistry 1993;100:431–440. [PubMed: 7512949]
40. Agalliu D, Schieren I. Heterogeneity in the developmental potential of motor neuron progenitors revealed by clonal analysis of single cells in vitro. Neural Dev 2009;4:2. [PubMed: 19123929]

41. Hanson MG, Landmesser LT. Normal patterns of spontaneous activity are required for correct motor axon guidance and the expression of specific guidance molecules. Neuron 2004;43:687–701. [PubMed: 15339650]

42. Luria V, Krawchuk D, Jessell TM, Laufer E, Kania A. Specification of motor axon trajectory by ephrin-B:EphB signaling: symmetrical control of axonal patterning in the developing limb. Neuron 2008;60:1039–1053. [PubMed: 19109910]

43. Luria V, Laufer E. Lateral motor column axons execute a ternary trajectory choice between limb and body tissues. Neural Dev 2007;2:13. [PubMed: 17605791]

44. Nieuwkoop, PD.; Faber, J. Normal table of Xenopus laevis. Amsterdam, The Netherlands: North Holland Publishing Co.; 1967.

45. Vonica A, Gumbiner BM. Zygotic Wnt activity is required for Brachyury expression in the early Xenopus laevis embryo. Dev. Biol 2002;250:112–127. [PubMed: 12297100]

46. Taylor MF, Paulauskis JD, Weller DD, Kobzik L. In vitro efficacy of morpholino-modified antisense oligomers directed against tumor necrosis factor-alpha mRNA. J. Biol. Chem 1996;271:17445–17452. [PubMed: 8663413]

47. Wilson PA, Melton DA. Mesodermal patterning by an inducer gradient depends on secondary cell-cell communication. Curr. Biol 1994;4:676–686. [PubMed: 7953553]

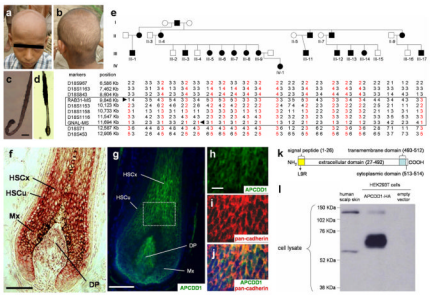

Figure 1. The HHS phenotype maps on chromosome 18p11.2 in a point mutation in *APCDD1* gene

a-d, Clinical appearance of HHS patients (**a, b**) and their hair shaft (**c, d**). Scale bar: 100 μm. **e**, Haplotype analysis of a Pakistani family HHS1. The linked haplotype is indicated in red. The critical recombination events are indicated by black arrowheads. **f**, *In situ* hybridization with *APCDD1* antisense mRNA probe in human hair follicles (HFs). *APCDD1* is present in the dermal papilla (DP), matrix (Mx), hair shaft cortex (HSCx), and cuticle (HSCu) of the HF. **g-j**, Immunofluorescence in human HFs with a mouse polyclonal anti-APCDD1 antibody (Abnova). The expression of APCDD1 protein in the HSCx [white boxed in (**g**)] overlaps with that of E- and P-cadherins (**h-j**).
Counterstaining with DAPI is shown in blue (**g, j**). Scale bars: 100 μm (**f, g**), 20 μm (**h**). **k**, Schematic of APCDD1 protein and the position of L9R mutation. **l**, A western blot with the mouse polyclonal anti-APCDD1 antibody (Abnova) from cell lysates of human scalp skin shows two fragments around 58 and 130 KDa in size. A similar pattern was observed with the HA-tagged wild-type APCDD1 overexpressed in HEK293T cells.

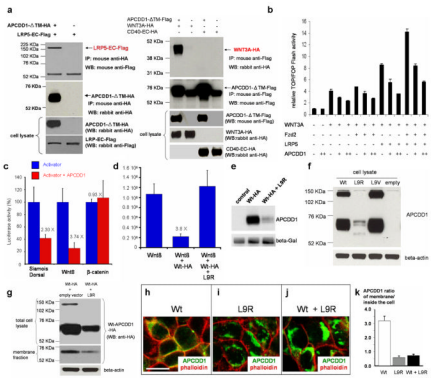

Figure 2. Wild-type, but not L9R mutant APCDD1, inhibits canonical Wnt signaling

a, Co-immunoprecipitation assays show that extracellular domain of APCDD1 (APCDD1ΔTM) strongly interacts with extracellular domain of LRP5 (LRP5-EC) and WNT3A. Extracellular domain of a non-Wnt related single transmembrane receptor CD40 (CD40-EC) was used as a negative control. **b**, TOP/FOP Flash reporter assays in HEK293T cells. **c**, Effect of APCDD1 overexpression on transcriptional activity of the Wnt-specific *Sia* reporter gene induced by Wnt8 or β-catenin *in Xenopus*. *APCDD1* (1 ng RNA) inhibited *Wnt8*-(50 pg RNA), but not β-*catenin*-induced (1 ng RNA) transcription. The number above the column indicates fold repression by APCDD1. **d**, The L9R mutant APCDD1 has a dominant negative effect on Wt APCDD1 in *Xenopus*. Activity of the *Sia* reporter gene induced by *Wnt8* RNA (50 pg) was inhibited by coinjection of Wt *APCDD1* RNA (1 ng), but not by coexpression of Wt and the L9R mutant. **e**, Western blot of the levels of APCDD1 in *Xenopus* embryos. L9R APCDD1 affects WT protein levels in *Xenopus* embryos. β-Gal is used as loading control. **f**, Western blot analysis of lysates from HEK293T cells transfected with Wt-, L9R- or L9V-APCDD1. **g**, The expression level of HA-tagged Wt-APCDD1 (Wt-HA) is decreased by co-expression with the L9R-APCDD1. β-actin was used as a normalization control (**f, g**). **h-j**, Immunofluorescence in transfected HEK293T with an APCCD1 antibody (green). Cell membrane was labeled with rhodaminephalloidin (red). Scale bar: 20 μm. **k**, Quantification of subcellular localization of APCDD1 isoforms. Bars represent mean ± 1 SEM (n = 20 cells per group). Wt versus L9R, $P < 8 \times 10^{-7}$; Wt versus Wt + L9R, $P < 3 \times 10^{-6}$; L9R versus Wt + L9R, P = 0.99. All P-values reported have the Bonferroni correction.

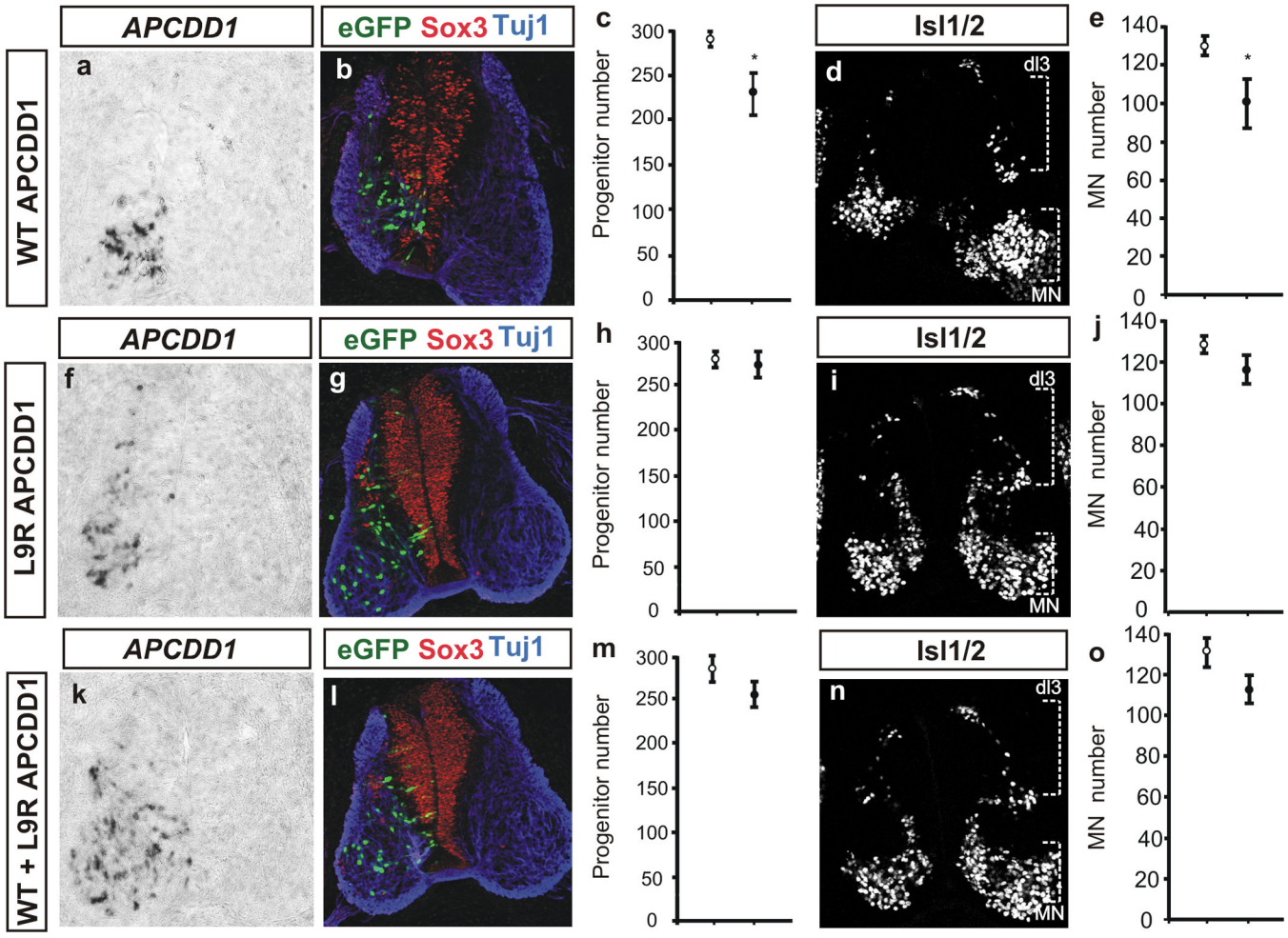

Figure 3. Overexpression of Wt-APCDD1, but not L9R mutant, inhibits progenitor proliferation and neuronal specification in the chick spinal cord

Transfection of Wt-, L9R- or both APCDD1 isoforms is visualized by eGFP fluorescence (**b, g, l;** green) and *in situ* for *hAPCDD1* (**a, f, k**). Sox3 labels neural progenitors in red and Tuj1 neurons in blue (**b, g, l**). Misexpression of Wt, but not L9R or a combination of both APCDD1 isoforms, reduces the number of $Sox3^+$ neural progenitors. Immunofluorescence for $Isl1/2^+$ (**d, i, n;** motor neurons MNs - ventral $Isl1/2^+$ cells; dI3 interneurons - dorsal $Isl1/2^+$ cells) shows that MNs are only reduced in the Wt APCDD1 electroporation. The D3 interneuron population is reduced in all conditions. Plots of $Sox3^+$ progenitors (**c, h, m**) and $Isl1/2^+$ MNs (**e, j, o**) in control (open circles) and transfected embryos (closed circles). Bars represent mean ± s.e.m. (n=40 embryos for WT-APCDD1, n=35 embryos for L9R-APCDD1 and n=28 embryos for WT- and L9R-APCDD1, Student's t-test, *$p<0.05$).

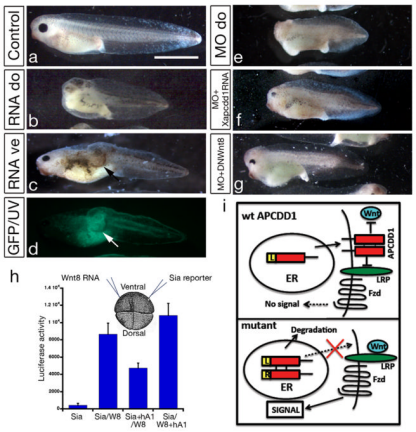

Figure 4. APCDD1 inhibits the Wnt pathway in *Xenopus* embryos

a, b, Dorsal overexpression of human APCDD1 (hAPCDD1) reduces axial and anterior structures (**b**). Scale bar: 4 mm (**a**). **c-d**, Ventral overexpression of hAPCDD1 produces a secondary axis (arrow in **c**) in cell autonomous fashion (GFP tracer, arrow in **d**). **e-g**, Phenotype of Xapcdd1 protein depletion and its rescue. Dorsal depletion by morpholino oligonucleotide (MO) produced a ventralized phenotype (**e**), rescued by *Xapcdd1* RNA (**f**) and dominant-negative *Wnt8* RNA (DN8) (**g**). **h**, APCDD1 is required in the signal-receiving cells. Wnt8 RNA and Siamois reporter gene were injected in adjacent cells. hAPCDD1 inhibited signaling only when coinjected with the reporter. **i**, Potential mechanism of action for wild-type and mutant APCDD1. Upper panel: wild type APCDD1 (L) is processed in the ER and localized at the cell membrane, where it may inhibit Wnt signaling by interacting with WNT and LRP proteins. Lower panel: when wild type and L9R-APCDD1 (R) are coexpressed, wild type APCDD1 is retained and degraded in the ER with the mutant, thus releasing Wnt signaling activity.